Progress In Electromagnetics Research, PIER 96, 37–62, 2009

THEORETICAL MODEL OF ELECTROMAGNETIC SCATTERING FROM 3D MULTI-LAYER DIELECTRIC MEDIA WITH SLIGHTLY ROUGH SURFACES

Z. W. Lin, X. J. Zhang, and G. Y. Fang

Institute of Electronics
Chinese Academy of Sciences
Beijing 100190, China

Abstract—A theoretical model of scattering from three-dimensional arbitrary layered media with 3D infinite rough surfaces based on the small perturbation method (SPM) is derived in the present paper. The scattering field and bistatic scattering coefficient for linear polarized waves are derived respectively. Firstly, the electric and magnetic fields in each region of the layered structure are expanded into perturbation series in spectral domain. Secondly, the expansion coefficients of each order are obtained by applying the boundary conditions. As a result, the expressions of the zeroth-, first- and second-order solutions of the scattering problem based on the SPM are obtained, in which the second-order solution is the primary contribution of this work. The theoretical model is helpful to understand the dependence between the scattering field and physical properties of the layered structure (such as surface roughness and dielectric constants at different depths). The result can be applied to modeling of the received radar signal from nature targets such as layered soil and ice with full polarizations.

1. INTRODUCTION

The problem of electromagnetic scattering from inhomogeneous media has been investigated for several decades [1–4]. The scattering models are applied to remote sensing, geoscience and optics. In recent years, a number of researches focus on scattering from inhomogeneous dielectric subsurface structure with rough interfaces considering the penetration property of electromagnetic waves. In the application of remote sensing, the scattering models are helpful for understanding

Corresponding author: Z. W. Lin (zhiweilin.mailbox@gmail.com).

the forward problem of scattering from natural targets such as layered soil, sea ice, ionosphere, lunar surface, etc. [1–10].

In terms of applications, the explicit closed-form solutions of the scattering problem are highly desirable, while the numerical methods have huge computational costs and can not reveal the internal relationship between the scattering patterns and the geometrical and physical parameters of the targets. When the penetration property of electromagnetic waves is taken into account, the wave number k is often small, thus kh and kl both are small numbers for slightly rough surfaces, where h and l are the rms height and correlation length of the rough surfaces respectively. In this case, a perturbation technique is often employed to solve the scattering problem [9].

The closed-form solutions of the scattering problem have been derived based on the first-order small perturbation method (SPM) in recent work. Fuks has investigated problem of electromagnetic wave scattering from an arbitrary layered medium with rough surfaces using an equivalent current model [6]. Sarabandi et al. have studied the radar response of a multi-layer dielectric media with a rough interface [7]. Franceschetti et al. have analyzed the connection between the existing first-order SPM solutions for the scattering from a layered structure with a rough interface and casted the existing first-order models in a unified compact formulation. Imperatore et al. have derived the solution of the problem of electromagnetic scattering from a layered structure with an arbitrary number of rough interfaces [9].

The first-order SPM solution gives explicit close-form analytical expressions. However, the first-order SPM solution is unable to characterize the cross-polarized backscattering which plays an important role in signal simulation of the scattering problem with full polarizations and parameter inversion of surface and subsurface structures (such as soil moisture for different depths of the subsurface structure and roughness of the surfaces) using polarimetric synthetic aperture radar (PolSAR). Cloude et al. have proposed an alternative way to introduce the cross-polarized backscattering into the first-order SPM solution by rotating a random angle to the plane perpendicular to the scattering plane [11], but the range and distribution of the random variables are unpredictable and need further discussion. In the framework of the perturbation technique, a recommended way to solve this problem is to derive the high-order solutions.

In this work, we derive the SPM solutions for the scattering from arbitrary layered media with 3D infinite rough surfaces up to the second order. The electric and magnetic fields in each region of the layered structure are expanded as a superposition of up- and down-going orthogonal polarized plane waves toward different directions of upper and lower half-space with unknown amplitudes in spectral domain. Since the interfaces in the subsurface structure are assumed to be planar, the generalized reflection coefficient is introduced to specify the reflection from the subsurface structure. The waves scattered by the rough surfaces are expanded into perturbation series with unknown coefficients. The expansion coefficient of each order is then solved by applying the boundary conditions. The scattering field in the far-field zone is approximated by the stationary phase method. Since we suppose the height profile of the rough surfaces is a Gaussian process, the coupling between the first- and second-order fields disappears when we calculate the bistatic scattering coefficient of the layered structure. As a result, the closed-form expressions of the scattering fields and bistatic scattering coefficients of the first- and second-order SPM solutions for the layered structure are obtained. Numerical samples are carried out to illustrate the contributions of zeroth-, first- and second-order of SPM solutions to the scattering pattern of the layered structure. The correction introduced by the second-order solution to the coherent reflected field of the layered structure is also illustrated.

2. PRELIMINARIES

2.1. Geometry

Figure 1 shows the 2D section of the proposed 3D problem. Regions 0 and n are half-spaces. The interface sandwiched between regions 0 and 1 is a 3D infinite rough boundary. Other interfaces are assumed to be planar and parallel with each other. Each region is

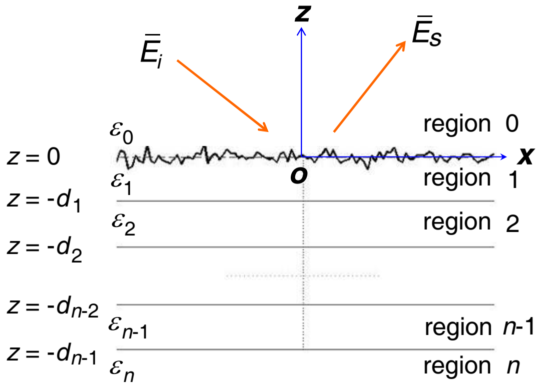

Figure 1. 2D slice of multi-layer dielectric media with rough surfaces.

a homogeneous medium with a dielectric constant ε_m, $m = 0, 1, \ldots, n$. The permeabilities of all regions are assumed equal to the permeability of free space. The wave number of each region is denoted by k_m, $m = 0, 1, \ldots, n$. The depth of the planar interface between regions m and $m+1$ is denoted by d_m, $m = 1, 2, \ldots, n-1$.

The surface profile is denoted by $z = g(x, y)$, where $g(x, y)$ is a Gaussian process with known statistical characteristics. The surface height profile is assumed to be statistically homogeneous. The rms height h and correlation length l of the rough surfaces are assumed to be small numbers compared to the incident wavelength to ensure the perturbation approximation to be carried out. However, the range of validity of the perturbation technique is out of the discussion of the present paper.

2.2. Problem Definition

In the following sections, the parameters with the superscript i are of the incident wave. The superscripts (or subscript) h and v denote the H polarization and V polarization. The subscript $\perp$ denotes the projection of the corresponding vector on plane $z = 0$. The subscripts x, y or z denotes the projection of the corresponding vector on x, y or z axis, respectively. The parameters with subscript m belong to region m, $m = 0, 1, \ldots, n$.

The plane wave incident on the layered structure from region 0 is

$$\bar{E}_0^i(\bar{r}) = e^{i\bar{k}_0^i \cdot \bar{r}} \hat{e}_0^i \tag{1}$$

where $\bar{r}$ is the position vector, $\bar{k}_0^i = \bar{k}_\perp^i - k_{0z}^i \hat{z} = k_x^i \hat{x} + k_y^i \hat{y} - k_{0z}^i \hat{z} = k_0 \hat{k}_0^i$; $k_0 = \sqrt{k_x^2 + k_y^2 + k_z^2}$ is the wave number of the incident wave; $\hat{k}_0^i$ is the unit vector of the incident direction; $\hat{e}_0^i$ is the unit polarization vector of the incident wave. Since the incident wave is a plane wave, $\hat{k}_0^i$ is perpendicular to $\hat{e}_0^i$. We can decompose $\hat{e}_0^i$ into two perpendicular unit vectors in the plane perpendicular to the direction of $\hat{k}_0^i$

$$\hat{e}_0^i = e_0^h \hat{h}\left(-k_{0z}^i\right) + e_0^v \hat{v}\left(-k_{0z}^i\right) \tag{2}$$

where

$$e_0^h = \hat{e}_0^i \cdot \hat{h}\left(-k_{0z}^i\right), \quad e_0^v = \hat{e}_0^i \cdot \hat{v}\left(-k_{0z}^i\right) \tag{3}$$

and

$$\begin{aligned}\hat{h}\left(-k_{0z}^{i}\right) &= \frac{\hat{k}_0^i \times \hat{z}}{\left|\hat{k}_0^i \times \hat{z}\right|} = \frac{k_y^i \hat{x} - k_x^i \hat{y}}{k_\perp^i}, \\ \hat{v}\left(-k_{0z}^{i}\right) &= \hat{h}\left(-k_{0z}^{i}\right) \times \hat{k}_0^i = \frac{k_\perp^i}{k_0}\hat{z} + \frac{k_{0z}}{k_0 k_\perp^i}\left(k_x^i \hat{x} + k_y^i \hat{y}\right)\end{aligned} \tag{4}$$

$\hat{h}(-k_{0z}^i)$ and $\hat{v}\left(-k_{0z}^i\right)$ are the unit vectors of H and V polarized components of the incident wave. $\hat{k}_0^i$, $\hat{v}\left(-k_{0z}^i\right)$ and $\hat{h}\left(-k_{0z}^i\right)$ form an orthogonal set. The time factor $e^{-j\omega t}$ is understood.

The electric and magnetic fields at the point $\bar{r}$ in region m can be represented as a superposition of up- and down-going orthogonal polarized waves in spectral domain [7]

$$\begin{aligned}\bar{E}_m(\bar{r}) = \int_{-\infty}^{+\infty} d\bar{k}_\perp \Big\{ &\left[f_{mh}^{+}\hat{h}_m(k_{mz}) + f_{mv}^{+}\hat{v}_m(k_{mz})\right] e^{ik_{mz}z} \\ &+ \left[f_{mh}{-}\hat{h}_m(-k_{mz}) + f_{mv}{-}\hat{v}_m(-k_{mz})\right] e^{-ik_{mz}z}\Big\} e^{i\bar{k}_\perp\cdot\bar{r}_\perp}\end{aligned} \tag{5}$$

$$\begin{aligned}\bar{H}_m(\bar{r}) = \frac{1}{\eta_m}\int_{-\infty}^{+\infty} d\bar{k}_\perp \Big\{ &\left[-f_{mh}^{+}\hat{v}_m(k_{mz}) + f_{mv}^{+}\hat{h}_m(k_{mz})\right] e^{ik_{mz}z} \\ &+ \left[-f_{mh}^{-}\hat{v}_m^{-}(-k_{mz}) + f_{mv}^{-}\hat{h}_m^{-}(-k_{mz})\right] e^{-ik_{mz}z}\Big\} e^{i\bar{k}_\perp\cdot\bar{r}_\perp}\end{aligned} \tag{6}$$

where $d\bar{k}_\perp = dk_x dk_y$; the superscripts $+$ and $-$ denote the up- and down-going waves respectively; $f_{mh}^{\pm}$ and $f_{mv}^{\pm}$ denote the unknown amplitudes of the up- and down-going waves of H and V polarizations in region m; η_m is the wave impedance of region m, $m = 0, 1, \ldots, n$. The unit vectors $\hat{h}(\pm k_{mz})$ and $\hat{v}(\pm k_{mz})$ are defined as

$$\hat{h}(\pm k_{mz}) = \frac{k_y\hat{x} - k_x\hat{y}}{k_\perp^i}, \quad \hat{v}(\pm k_{mz}) = \frac{k_\perp}{k_m}\hat{z} \mp \frac{k_{mz}}{k_m k_\perp}(k_x\hat{x} + k_y\hat{y}) \tag{7}$$

where $k_{mz} = \sqrt{k_m^2 - k_x^2 - k_y^2}$. The unknown amplitudes will be discussed in Section 3.

The boundary conditions at the mth interface satisfy

$$\hat{n}_m \times \left[\bar{E}_m(\bar{r}) - \bar{E}_{m+1}(\bar{r})\right]_m = 0, \; \hat{n}_m \times \left[\bar{H}_m(\bar{r}) - \bar{H}_{m+1}(\bar{r})\right]_m = 0 \tag{8}$$

$m = 0, 1, \ldots, n-1$, $\hat{n}_m$ denotes the normal vector of the mth interface

$$\hat{n}_0 = \frac{-g_x \hat{x} - g_y \hat{y} + \hat{z}}{\sqrt{1 + g_x^2 + g_y^2}}, \quad \hat{n}_m = \hat{z} \tag{9}$$

where $g_x = \partial g(x, y)/\partial x$ and $g_y = \partial g(x, y)/\partial y$, $m = 1, 2, \ldots, n-1$. Here we have assumed function $g(x, y)$ is derivable.

3. ANALYSES

In this section, we will determine the unknown amplitudes $f_{mh}^{\pm}$ and $f_{mv}^{\pm}$ by the boundary conditions and SPM. There are $4(n+1)$ unknown amplitudes which need to be solved. First, we determine the amplitudes of the incident wave. Then, we find the relationship of the unknown amplitudes of up- and down-going waves in the subsurface structure through the boundary conditions for the planar interfaces. Second, we solve the amplitudes of scattering waves by employing boundary condition for the rough surfaces and SPM. According to field expansions, we express the boundary conditions in spectral domain, and we obtain a linear equation set about the unknown amplitude with week form. Next, we expand the unknown amplitudes into perturbation series. The expansion coefficients of each order can be solved from the equation set after an order-matching procedure. As a result, the expansion coefficients of zeroth-, first- and second-order are derived. We then estimate the scattering field in the far-field zone using the zeroth-, first- and second-order approximation respectively. At last, we calculate the expression of the bistatic scattering coefficient of the layered structure.

3.1. The Amplitudes of the Incident Wave

We begin with the amplitude of the down-going wave in region 0. In region 0, the down-going wave is the incident wave. The amplitudes of the down-going wave f_{0h}^{-} and f_{0v}^{-} are found immediately from the Fourier transform of the incident wave (1).

$$f_{0h}^{-} = e_0^h \delta\left(\bar{k}_\perp - \bar{k}_\perp^i\right), \quad f_{0v}^{-} = e_0^v \delta\left(\bar{k}_\perp - \bar{k}_\perp^i\right) \tag{10}$$

where δ is the Dirac function.

3.2. The Amplitudes of the Waves in the Subsurface Structure

Since the interfaces of the subsurface structure are planes (see Fig. 1), the Fresnel law holds at each interface, and the amplitudes of up- and down-going waves in region 1 to n are not independent. In region 1 we have

$$f_{1h}^{+} = \mathbf{R}_1^h e^{2ik_{1z}d_1} f_{1h}^{-}, \quad f_{1v}^{+} = \mathbf{R}_1^v e^{2ik_{1z}d_1} f_{1v}^{-} \tag{11}$$

where $\mathbf{R}_1^h$ and $\mathbf{R}_1^v$ are the generalized reflection coefficients [8] for H and V polarizations at the 1st interface. The definition of the generalized reflection coefficient is presented in Appendix A. Since the physical parameters of the layered structure are known, the generalized reflection coefficients can be calculated easily. Further, the amplitudes of the down-going waves for H and V polarizations in region m $(m = 2, 3, \ldots, n)$ can be represented as functions of f_{1h}^{-} and f_{1v}^{-}

$$\begin{aligned} f_{mh}^{-} &= T_1^h T_2^h \ldots T_{m-1}^h e^{ik_{1z}\Delta_1} e^{ik_{2z}\Delta_2} \ldots e^{ik_{(m-1)z}\Delta_{m-1}} f_{1h}^{-}, \\ f_{mv}^{-} &= T_1^v T_2^v \ldots T_{m-1}^v e^{ik_{1z}\Delta_1} e^{ik_{2z}\Delta_2} \ldots e^{ik_{(m-1)z}\Delta_{m-1}} f_{1v}^{-} \end{aligned} \tag{12}$$

where T_k^h and T_k^v are the Fresnel transmission coefficients, $\Delta_k = d_k - d_{k-1}$, $k = 1, 2, \ldots, n-1$. The up- and down-going waves in region m $(m = 2, 3, \ldots, n-1)$ also satisfy

$$f_{mh}^{+} = \mathbf{R}_m^h e^{2ik_{mz}\Delta_m} f_{mh}^{-}, \quad f_{mv}^{+} = \mathbf{R}_m^v e^{2ik_{mz}\Delta_m} f_{mv}^{-} \tag{13}$$

where $\mathbf{R}_m^h$ and $\mathbf{R}_m^v$ are the generalized reflection coefficients at the mth interface. Region n is a half space, and no source is located in this region, so the amplitudes of the up-going waves equal to zero, i.e., $f_{nh}^{+} = 0$ and $f_{nv}^{+} = 0$.

3.3. The Zeroth-, First- and Second-order SPM Solutions of the Amplitudes of the Scattering Wave

We have determined the exact expressions or the relationships of the $4n$ unknown amplitudes from the above discussion. The 4 residual unknown amplitudes f_{0h}^{+}, f_{0v}^{+}, f_{1h}^{-} and f_{1v}^{-} are independent variables. We will deal with those variables using the boundary conditions at the rough interface. Substituting the field expansion expressions (5) and (6) into the boundary conditions of the rough interface (8) and taking into account of (10) and (11), we obtain two linear vector equations with weak form

$$\begin{aligned} &\hat{n}_0 \times \Big\{ \Big[f_{0h}^{+} \hat{h}(k_{0z}) + f_{0v}^{+} \hat{v}(k_{0z}) \Big] e^{ik_{0z} g(\bar{r}_\perp)} \\ &\quad + \Big[e_0^h \delta\left(\bar{k}_\perp - \bar{k}_\perp^i\right) \hat{h}(-k_{0z}) + e_0^v \delta\left(\bar{k}_\perp - \bar{k}_\perp^i\right) \hat{v}(-k_{0z}) \Big] e^{-ik_{0z} g(\bar{r}_\perp)} \Big\} \\ &= \hat{n}_0 \times \Big\{ \Big[f_{1h}^{-} \mathbf{R}_1^h e^{2ik_{1z}d_1} \hat{h}(k_{1z}) + f_{1v}^{-} \mathbf{R}_1^v e^{2ik_{1z}d_1} \hat{v}(k_{1z}) \Big] e^{ik_{1z} g(\bar{r}_\perp)} \\ &\quad + \Big[f_{1h}^{-} \hat{h}(-k_{1z}) + f_{1v}^{-} \hat{v}(-k_{1z}) \Big] e^{-ik_{1z} g(\bar{r}_\perp)} \Big\} \end{aligned} \tag{14}$$

$$\begin{aligned}
&\hat{n}_0 \times \frac{1}{\eta_0}\Big\{\Big[-f_{0h}^{+}\hat{v}\left(k_{0z}\right)+f_{0v}^{+}\hat{h}\left(k_{0z}\right)\Big]\,e^{ik_{0z}g(\bar{r}_\perp)}\\
&\quad+\Big[-e_0^h\delta\left(\bar{k}_\perp-\bar{k}_\perp^i\right)\hat{v}\left(-k_{0z}\right)+e_0^v\delta\left(\bar{k}_\perp-\bar{k}_\perp^i\right)\hat{h}\left(-k_{0z}\right)\Big]\,e^{-ik_{0z}g(\bar{r}_\perp)}\Big\}\\
&=\hat{n}_0\times\frac{1}{\eta_1}\Big\{\Big[-\mathbf{R}_1^h e^{2ik_{1z}d_1}f_{1h}^{-}\hat{v}\left(k_{1z}\right)+\mathbf{R}_1^v e^{2ik_{1z}d_1}f_{1v}^{-}\hat{h}\left(k_{1z}\right)\Big]\,e^{ik_{1z}g(\bar{r}_\perp)}\\
&\quad+\Big[-f_{1h}^{-}\hat{v}\left(-k_{1z}\right)+f_{1v}^{-}\hat{h}\left(-k_{1z}\right)\Big]\,e^{-ik_{1z}g(\bar{r}_\perp)}\Big\}
\end{aligned}\tag{15}$$

(14) and (15) are the boundary conditions in spectral domain and can be written as six linear scalar equations for x, y and z directions. Note that the linear scalar equations for x and y directions are independent, and they are listed in Appendix B. The linear scalar equations for z directions are not independent, and we will not present them here.

The equation set (14) and (15) can be solved directly, but the solution is hard to be used in further calculations such as estimating the scattering fields and bistatic scattering coefficients of the scattering problem. An alternative way is to apply the SPM to carry out an approximated solution of the equation set. We expand the unknown amplitudes f_{0h}^{+}, f_{0v}^{+}, f_{1h}^{-} and f_{1v}^{-} into perturbation series

$$f_{0h,v}^{+}=\sum_{l=0}^{+\infty}f_{0h,v}^{+(l)},\quad f_{1h,v}^{-}=\sum_{l=0}^{+\infty}f_{1h,v}^{-(l)}\tag{16}$$

where the superscript (l) represents the order of the expansion coefficient and expands the exponential items into the Taylor series

$$e^{\pm ik_{mz}g(x,y)}=\sum_{l=0}^{+\infty}\frac{1}{l!}\left[\pm ik_{mz}g\left(x,y\right)\right]^l\tag{17}$$

where $m = 0$ or 1. We then determine the unknown expansion coefficient of each order through the equation set. Under the assumption of small roughness, the first several terms of the expansion give good approximation to solution of the problem. In the following, we will derive the zeroth-, first-, and second-order perturbation solutions of the problem.

Substituting (16) and (17) into (14) and (15), balancing the zeroth-order terms of the equation set, a matrix equation is obtained

$$\mathbf{A}\mathbf{x}_0=\mathbf{b}_0\tag{18}$$

where

$$\mathbf{A}=\begin{bmatrix} \frac{k_x}{k_\perp} & \frac{k_y k_{0z}}{k_\perp k_0} & -\frac{k_x}{k_\perp}\left(1+\mathbf{R}_1^h e^{2ik_{1z}d}\right) & \frac{k_y k_{1z}}{k_\perp k_1}\left(1-\mathbf{R}_1^v e^{2ik_{1z}d}\right) \\ \frac{k_y}{k_\perp} & -\frac{k_x k_{0z}}{k_\perp k_0} & -\frac{k_y}{k_\perp}\left(1+\mathbf{R}_1^h e^{2ik_{1z}d}\right) & -\frac{k_x k_{1z}}{k_\perp k_1}\left(1-\mathbf{R}_1^v e^{2ik_{1z}d}\right) \\ -\frac{k_y k_{0z}}{\eta_0 k_\perp k_0} & \frac{k_x}{\eta_0 k_\perp} & -\frac{k_y k_{1z}}{\eta_1 k_\perp k_1}\left(1-\mathbf{R}_1^h e^{2ik_{1z}d}\right) & -\frac{k_x}{k_\perp \eta_1}\left(1+\mathbf{R}_1^v e^{2ik_{1z}d}\right) \\ \frac{k_x k_{0z}}{\eta_0 k_\perp k_0} & \frac{k_y}{\eta_0 k_\perp} & \frac{k_x k_{1z}}{\eta_1 k_\perp k_1}\left(1-\mathbf{R}_1^h e^{2ik_{1z}d}\right) & -\frac{k_y}{k_\perp \eta_1}\left(1+\mathbf{R}_1^v e^{2ik_{1z}d}\right) \end{bmatrix} \tag{19}$$

$$\mathbf{x_0}=\begin{bmatrix} f_{0h}^{+(0)} \\ f_{0v}^{+(0)} \\ f_{1h}^{-(0)} \\ f_{1v}^{-(0)} \end{bmatrix},\ \mathbf{b_0}=\begin{bmatrix} -\left(\frac{k_x}{k_\perp}e_0^h-\frac{k_y k_{0z}}{k_\perp k_0}e_0^v\right)\delta\left(\bar{k}_\perp-\bar{k}_\perp^i\right) \\ -\left(\frac{k_y}{k_\perp}e_0^h+\frac{k_x k_{0z}}{k_\perp k_0}e_0^v\right)\delta\left(\bar{k}_\perp-\bar{k}_\perp^i\right) \\ -\frac{1}{\eta_0}\left(\frac{k_y k_{0z}}{k_\perp k_0}e_0^h+\frac{k_x}{k_\perp}e_0^v\right)\delta\left(\bar{k}_\perp-\bar{k}_\perp^i\right) \\ -\frac{1}{\eta_0}\left(-\frac{k_x k_{0z}}{k_\perp k_0}e_0^h+\frac{k_y}{k_\perp}e_0^v\right)\delta\left(\bar{k}_\perp-\bar{k}_\perp^i\right) \end{bmatrix} \tag{20}$$

The solution of (18) is

$$\begin{aligned} f_{0h}^{+(0)} &= \mathbf{R}_0^h e_0^h \delta\left(\bar{k}_\perp-\bar{k}_\perp^i\right), \quad f_{0v}^{+(0)} = \mathbf{R}_0^v e_0^v \delta\left(\bar{k}_\perp-\bar{k}_\perp^i\right) \\ f_{1h}^{-(0)} &= \mathbf{T}_0^h e_0^h \delta\left(\bar{k}_\perp-\bar{k}_\perp^i\right), \quad f_{1h}^{-(0)} = \mathbf{T}_0^v e_0^v \delta\left(\bar{k}_\perp-\bar{k}_\perp^i\right) \end{aligned} \tag{21}$$

where

$$\mathbf{T}_0^h=\frac{T_0^h}{1+\mathbf{R}_0^h\mathbf{R}_1^h e^{i2k_{1z}\Delta_1}}, \quad \mathbf{T}_0^v=\frac{\eta_1}{\eta_0}\frac{T_0^v}{1+\mathbf{R}_0^v\mathbf{R}_1^v e^{i2k_{1z}\Delta_1}} \tag{22}$$

are the total transmission coefficients at the zeroth interface. The zeroth-order solution in (21) is the generalized reflection coefficients of the layered structure with planar surfaces and total transmission coefficients of the planar surfaces. Note that the zeroth-order solution is the coherent component of the scattering problem.

Matching the first-order terms of the equation set, a matrix equation for the first-order terms is established

$$\mathbf{A}\mathbf{x}_1=\mathbf{b}_1 \tag{23}$$

where $\mathbf{A}$ is defined by (19) and

$$\mathbf{x}_1=\begin{bmatrix} f_{0h}^{+(1)} & f_{0v}^{+(1)} & f_{1h}^{-(1)} & f_{1v}^{-(1)} \end{bmatrix}^T,\ \mathbf{b}_1=\begin{bmatrix} b_{11} & b_{12} & b_{13} & b_{14} \end{bmatrix}^T \tag{24}$$

The superscript T denotes the operator of matrix transpose. The expression of $\mathbf{b}_1$ is presented in Appendix C. The first-order solution is

$$\begin{aligned} f_{0h,v}^{+(1)} &= \left[\tilde{f}_{0pp}^{+(1)} + \tilde{f}_{0pq}^{+(1)}\right]\left[iG\left(\bar{k}_\perp - \bar{k}_\perp^i\right)\right], \\ f_{1h,v}^{-(1)} &= \left[\tilde{f}_{1pp}^{-(1)} + \tilde{f}_{1pq}^{-(1)}\right]\left[iG\left(\bar{k}_\perp - \bar{k}_\perp^i\right)\right] \end{aligned} \tag{25}$$

where $p, q = H, V$ and $p \neq q$. The expressions of $\tilde{f}_{0pp}^{+(1)}$, $\tilde{f}_{0pq}^{+(1)}$, $\tilde{f}_{1pp}^{-(1)}$ and $\tilde{f}_{1pq}^{-(1)}$ are amplitudes for co-polarized and cross-polarized waves, and they are presented in Appendix D. $G\left(\bar{k}_\perp\right)$ is the Fourier transform of the surface height profile $g(x, y)$

$$G\left(\bar{k}_\perp\right) = \int_{-\infty}^{+\infty}\int_{-\infty}^{+\infty} dxdy\left[g(x, y)\, e^{-i(k_x x + k_y y)}\right] \tag{26}$$

The above results for the zeroth- and first-order solutions correspond to expressions in [6]. The first-order solution of the scattering problem stands for the contribution of single scattering component of the structure, which contains the primary incoherent scattering component. The mechanism of single scattering is illustrated in Fig. 2.

Next, we determine the second-order terms through the equation set. The matrix equation for the second-order solution can be written as

$$\mathbf{A}\mathbf{x}_2 = \mathbf{b}_2 \tag{27}$$

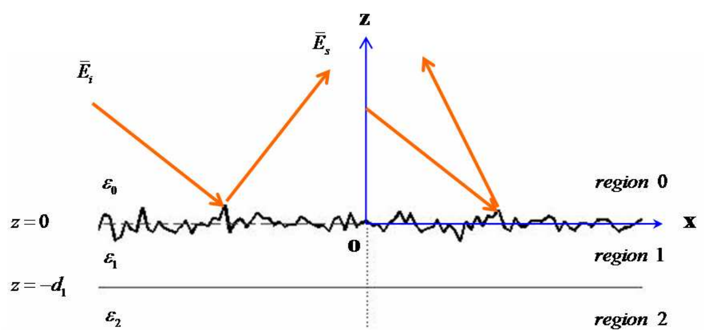

Figure 2. Illustration of single scattering.

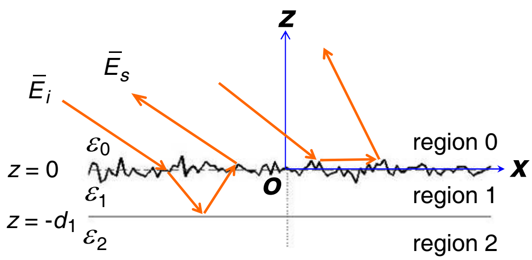

Figure 3. Illustration of double-scattering.

where

$$\mathbf{x}_2 = \begin{bmatrix} f_{0h}^{+(2)} & f_{0v}^{+(2)} & f_{1h}^{-(2)} & f_{1v}^{-(2)} \end{bmatrix}^T, \ \mathbf{b}_2 = \begin{bmatrix} b_{21} & b_{22} & b_{23} & b_{24} \end{bmatrix}^T \tag{28}$$

The expression of $\mathbf{b}_2$ is presented in Appendix C. Because we are concerned about the scattering fields for linear polarizations HH, VH, HV and VV in region 0, we only calculate $f_{0hh}^{+(2)}$, $f_{0vh}^{+(2)}$, $f_{0hv}^{+(2)}$ and $f_{0vv}^{+(2)}$. The solution is

$$f_{0pq}^{+(2)} = \int_{-\infty}^{+\infty} d\bar{\kappa}_\perp G\left(\bar{k}_\perp - \bar{\kappa}_\perp\right) G\left(\bar{\kappa}_\perp - \bar{k}_\perp^i\right) \tilde{f}_{0pq}^{+(2)}\left(\bar{\kappa}_\perp\right) \tag{29}$$

where $p, q = H, V$, $\bar{\kappa}_\perp$ is a dummy variable, $d\bar{\kappa}_\perp = d\kappa_x d\kappa_y$. The expressions of $f_{0pq}^{+(2)}$ are presented in Appendix D.

It is easy to validate that the degraded forms of (29) for the simple case of single rough surfaces coincide with the result on [12]. The second-order solutions contribute to the double-bounce component of the layered structure, which is illustrated in Fig. 3. The mechanism of the double-bounce scattering makes the primary contribution to the cross-polarized component especially in the case of backscattering. Since the generalized reflection coefficients are involved in the zeroth-, first- and second-order solutions, the results can be used to deal with the structure with an arbitrary number of layers.

3.4. The Scattering Fields and the Bistatic Scattering Coefficients

The scattering field $\bar{E}_0(\bar{r})$ in region 0 can be approximated as

$$\bar{E}_0(\bar{r}) \simeq \bar{E}_0^{(0)}(\bar{r}) + \bar{E}_0^{(1)}(\bar{r}) + \bar{E}_0^{(2)}(\bar{r}) \tag{30}$$

where $\bar{E}_0^{(0)}(\bar{r})$, $\bar{E}_0^{(1)}(\bar{r})$ and $\bar{E}_0^{(2)}(\bar{r})$ are scattering field of the zeroth-, first- and second-order SPM solutions respectively

$$\bar{E}_0^{(0)} = \mathbf{R}_0^{hi} e_0^h \hat{h}\left(-k_{0z}^i\right) + \mathbf{R}_0^{vi} e_0^v \hat{v}\left(-k_{0z}^i\right) \tag{31}$$

$$\bar{E}_0(1)(\bar{r}) = \int_{-\infty}^{+\infty} d\bar{k}_\perp \left[f_{0h}^{+(1)} \hat{h}_0(k_{0z}) + f_{0v}^{+(1)} \hat{v}_0(k_{0z})\right] e^{i\left(k_{0z}z + \bar{k}_\perp \cdot \bar{r}_\perp\right)} \tag{32}$$

$$\bar{E}_0^{(2)}(\bar{r}) = \int_{-\infty}^{+\infty} d\bar{k}_\perp \left[f_{0h}^{+(2)} \hat{h}_0(k_{0z}) + f_{0v}^{+(2)} \hat{v}_0(k_{0z})\right] e^{i\left(k_{0z}z + \bar{k}_\perp \cdot \bar{r}_\perp\right)} \tag{33}$$

Note that the zeroth-order field $\bar{E}_0^{(0)}(\bar{r})$ exists only in the specular direction.

In the far-field zone, the scattering field can be estimated by the stationary phase method. We have

$$E_{0pq}^{(l)}(\bar{r}) \simeq -\frac{e^{ik_0 r}}{r} i2\pi k_0 \cos\theta f_{0pq}^{+(l)} e_0^q \tag{34}$$

where $l = 1, 2$, $p, q = H, V$. θ is the angle between the scattering wave and z axis.

The bistatic scattering coefficient is defined as the ratio of the scattering power of polarization p per unit solid angle in the scattering direction to the scattering power averaged over 4π radians

$$\gamma_{pq}\left(\bar{k}_\perp \bar{k}_\perp^i\right) = \lim_{\substack{A\to+\infty \\ r\to+\infty}} \frac{4\pi r^2 \left\langle \left|\bar{E}_0(\bar{r}) \cdot \hat{p}\right|^2 \right\rangle}{A \left|e_0^q\right|^2 \cos\theta^i} \tag{35}$$

where $\bar{k}_\perp^i$ and $\bar{k}_\perp$ denote the directions of the incident wave and scattering wave respectively; A is the area illustrated by the incident wave; θ^i is the angle between the incident wave and z axis; the symbol $\langle\rangle$ denotes the operator of ensemble average. Since $g(x, y)$ is a Gaussian random process, the Fourier transformation $G\left(\bar{k}_\perp\right)$ is also Gaussian. For a jointly Gaussian random vector $\{G_1, G_2, G_3, G_4\}$, the following identities hold

$$\langle G_1 G_2 G_3 \rangle = 0,\ \langle G_1 G_2 G_3 G_4 \rangle = \langle G_1 G_2 \rangle + \langle G_2 G_3 \rangle + \langle G_3 G_4 \rangle + \langle G_1 G_4 \rangle \tag{36}$$

The ensemble average of the incoherent scattering field can be written as

$$\left\langle \bar{E}_0(\bar{r}_1) \bar{E}_0(\bar{r}_2)^* \right\rangle \simeq \left\langle \bar{E}_0^{(1)}(\bar{r}_1) \bar{E}_0^{(1)}(\bar{r}_2)^* \right\rangle + \left\langle \bar{E}_0^{(2)}(\bar{r}_1) \bar{E}_0^{(2)}(\bar{r}_2)^* \right\rangle \tag{37}$$

Therefore the bistatic scattering coefficient can be approximate by [12]

$$\gamma_{pq}\left(\bar{k}_\perp, \bar{k}_\perp^i\right) \simeq \gamma_{pq}^{(1)}\left(\bar{k}_\perp, \bar{k}_\perp^i\right) + \gamma_{pq}^{(2)}\left(\bar{k}_\perp, \bar{k}_\perp^i\right) \tag{38}$$

where

$$\gamma_{pq}^{(1)}\left(\bar{k}_\perp, \bar{k}_\perp^i\right) = \frac{4\pi k_0^2 \cos^2\theta}{\cos\theta^i} \left|\tilde{f}_{0pq}^{+(1)}\right|^2 W\left(\bar{k}_\perp - \bar{k}_\perp^i\right) \tag{39}$$

$$\gamma_{pq}^{(2)}\left(\bar{k}_\perp, \bar{k}_\perp^i\right) = \frac{4\pi k_0^2 \cos^2\theta}{\cos\theta^i} \int_{-\infty}^{+\infty} d\bar{\kappa}_\perp W\left(\bar{k}_\perp - \bar{\kappa}_\perp\right) W\left(\bar{\kappa}_\perp - \bar{k}_\perp^i\right) \tilde{f}_{0pq}^{+(2)}\left(\bar{\kappa}_\perp\right)\left[\tilde{f}_{0pq}^{+(2)}\left(\bar{\kappa}_\perp\right) + \tilde{f}_{0pq}^{+(2)}\left(\bar{k}_\perp - \bar{\kappa}_\perp + \bar{k}_\perp^i\right)\right]^* \tag{40}$$

$*$ is the operator of conjugation and

$$W\left(\bar{k}_\perp\right) = \lim_{A\to\infty} \frac{\left\langle \left|G\left(\bar{k}_\perp\right)\right|^2 \right\rangle}{A} \tag{41}$$

is the spectral density function of the height profile $g\left(x, y\right)$.

4. NUMERICAL SAMPLES

The expressions of the zeroth- and first-order solutions derived above coincide with the result in [6]. To validate the expressions of the bistatic scattering coefficients of the second-order SPM solution, we reproduce the curve of 2-2 term of Figure 3 in [13] for the simple case of single rough surfaces, which is shown in Fig. 4. The correlation

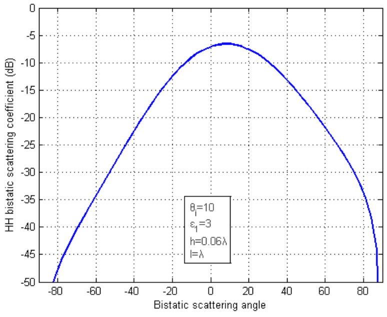

Figure 4. Reproducing the result on [13].

function of the rough surfaces is assumed to be a Gaussian form

$$\rho\left(\bar{r}_{\perp}\right) = e^{-\left|\bar{r}_{\perp}\right|^2/l^2} \tag{42}$$

and the corresponding spectral density function is

$$W\left(\bar{k}_{\perp}\right) = \frac{h^2 l^2}{4\pi} e^{-\left|\bar{k}_{\perp}\right|^2 l^2/4} \tag{43}$$

Without loss of generality, we consider a two-layer structure in the following discussion. Fig. 5(a) exhibits the difference of the

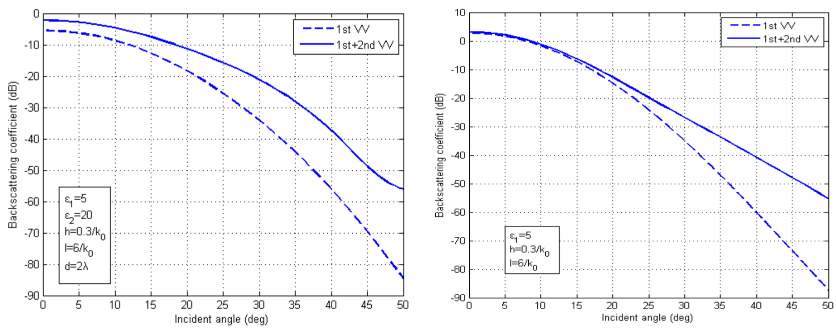

(a) (b)

Figure 5. Backscattering from a two-layer structure and a one-layer structure using the first and the combination of the first and second orders of the SPM solutions.

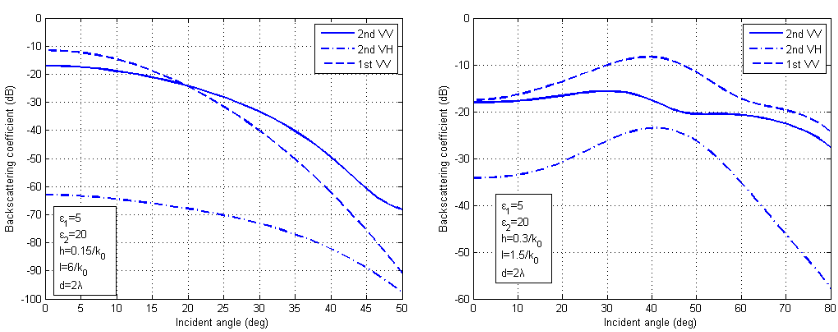

(a) (b)

Figure 6. Backscattering from two-layer structures with different roughness.

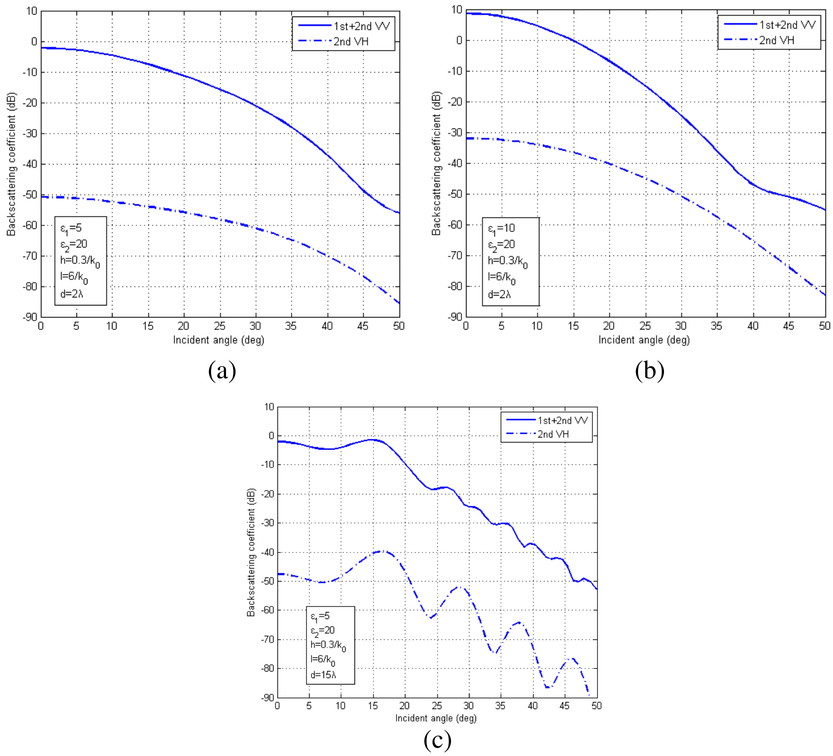

Figure 7. Backscattering from two-layer structures with different ε_1 and d_1.

VV polarized backscattering from the two-layer structure between the first- and the combination of the first- and second-order SPM solutions. Under the roughness of Fig. 5, the contribution of the double-bounce component is considerable for VV polarization. We see as the incident angle increases, the double-bounce component provides more co-polarized backscattering power than the single-scattering component. Compared with Fig. 5(b), the contribution of the double-bounce component in a layered structure (Fig. 5(a)) is more than the contribution of double-bounce component in a single layer structure, especially in the case of small incident angle. However, as the roughness increases, i.e., the rms height h becomes large, and the correlation length l becomes small, the backscattering power increases, and the contribution of the single-scattering component is dominating, which is illustrated in Figs. 6(a) and (b). The increase

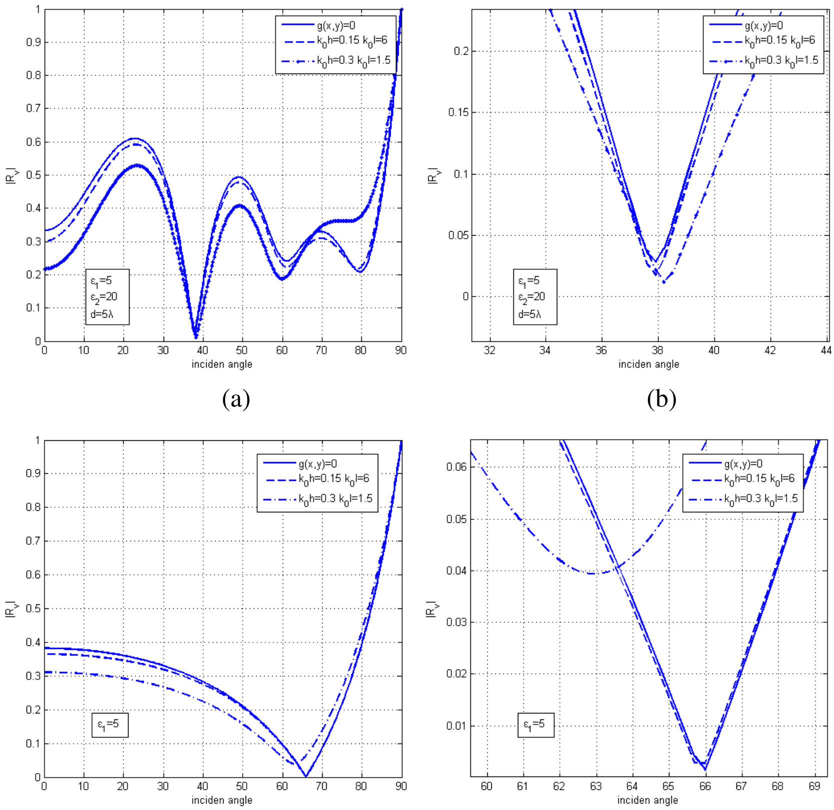

(a) (b)

(c) (d)

Figure 8. Ratio of the amplitude of the coherent reflected wave from a two-layer structure and a one-layer structure with different roughness and the incident wave of VV polarization.

in the surface roughness also results in a significant enhancement in the cross-polarized component. Figs. 7(a) and (b) show when the dielectric constant of the upper layer changes, the backscattering power changes consequently. The cross-polarized component is more sensitive to the variation of dielectric constant than co-polarized one. Fig. 7(c) shows the oscillation behavior of the backscattering from a two-layer structure. It is noted that the oscillation behavior of the cross-polarized component in Fig. 7(c) is more significant than co-polarized one.

Figure 8 shows the ratio of the amplitude of coherent reflected wave from a two-layer structure with different roughness and incident wave. When the roughness of the surfaces is small, the ratio is close to the reflection coefficient of the layered structure with a planar surface. The amplitude of the ratio is less than the reflection coefficient, because a part of the incident power is scattered into different directions by the rough surfaces. When the incident angle is close to 90 degree, the ratio is more than the reflection coefficient due to the contribution introduced by the double-bounce component. The Brewster-like effect of the layered structure is also observed in Fig. 8. The shift of the Brewster angle is shown clearly in Fig. 8(b). As the roughness of the surfaces increases, the shift of the Brewster angle is positive. For a one-layer structure, however, according to the perturbation technique, the shift is always negative [14], which is shown in Figs. 8(c) and (d).

5. CONCLUSION

A theoretical model of the scattering from a three-dimensional arbitrary layered media with slightly infinite rough surfaces based on the SPM is investigated in this work. The expressions of the zeroth-, first- and second-order SPM solutions for the layered structure are derived, in which the second-order solution is the primary contribution of this work. The expressions of the second-order scattering field and corresponding bistatic scattering coefficient result in integral forms. However, the integral for variable $\bar{\kappa}_{\perp}$ is well behaved, so numerical integration can be carried out without difficulty. The expressions are validated by comparing with the known results. According to the numerical results, the cross-polarized backscattering component is more sensitive to the variation of the physical parameters of the layered structure than the co-polarized backscattering component. The Brewster-like effect and shift of the reflection coefficient introduced by the second-order SPM solution are also observed.

The contributions of high-order SPM solutions for the layered structure are still unknown. It can be predicted when the number of rough interfaces of a layered structure is more than one, the coupling effect of rough interfaces will be enhanced, and the contribution of high-order terms will increase. Our future work will focus on the second and higher order SPM solutions for a layered structure with arbitrary number of rough interfaces and the numerical simulations of the scattering from a layered structure with rough interfaces.

ACKNOWLEDGMENT

This work is support by The National High Technology Research and Development Program ("863" Program) of China (Project

No. 2009AA12Z132) and National Nature Science Foundation of China (Project No. 60890071).

APPENDIX A. THE GENERALIZED REFLECTION COEFFICIENTS

The Fresnel reflection and transmission coefficients for H and V polarized waves at the mth interface are defined as follows [8]

$$R_m^h = \frac{k_{mz} - k_{(m+1)z}}{k_{mz} + k_{(m+1)z}}, \quad R_m^v = \frac{\varepsilon_{(m+1)z} k_{mz} - \varepsilon_{mz} k_{(m+1)z}}{\varepsilon_{(m+1)z} k_{mz} + \varepsilon_{mz} k_{(m+1)z}} \tag{A1}$$

$$T_m^h = \frac{2k_{mz}}{k_{mz} + k_{(m+1)z}}, \quad T_m^v = \frac{2\varepsilon_{(m+1)z} k_{mz}}{\varepsilon_{(m+1)z} k_{mz} + \varepsilon_{mz} k_{(m+1)z}} \tag{A2}$$

where $m = 0, 1, \ldots, n-1$. The Fresnel reflection and transmission coefficients satisfy $T_m^p = 1 + R_m^p$ with $p = H$ or V.

The generalized reflection coefficients for H and V polarized waves at the mth interface have the recursive relations [8]

$$\begin{aligned} \mathbf{R}_m^h &= \frac{\mathbf{R}_m^h + \mathbf{R}_{m+1}^h e^{i2k_{(m+1)z}\Delta_{m+1}}}{1 + \mathbf{R}_m^h \mathbf{R}_{m+1}^h e^{i2k_{(m+1)z}\Delta_{m+1}}}, \\ \mathbf{R}_m^v &= \frac{\mathbf{R}_m^v + \mathbf{R}_{m+1}^v e^{i2k_{(m+1)z}\Delta_{m+1}}}{1 + \mathbf{R}_m^v \mathbf{R}_{m+1}^v e^{i2k_{(m+1)z}\Delta_{m+1}}} \end{aligned} \tag{A3}$$

$$\begin{aligned} \mathbf{T}_m^h &= \frac{T_m^h}{1 + \mathbf{R}_m^h \mathbf{R}_{m+1}^h e^{i2k_{(m+1)z}\Delta_{m+1}}}, \\ \mathbf{T}_m^v &= \frac{\eta_{m+1}}{\eta_m} \frac{T_m^v}{1 + \mathbf{R}_m^v \mathbf{R}_{m+1}^v e^{i2k_{(m+1)z}\Delta_{m+1}}} \end{aligned} \tag{A4}$$

where $\Delta_{m+1} = d_{m+1} - d_m$, $m = 0, 1, \ldots, n-1$ with $\mathbf{R}_n^p = R_n^p$ $p = H$ or V.

APPENDIX B. THE EXPRESSION OF THE SCALAR EQUATION SET

Substituting (9) into (14) and (15) and changing the vector equations into scalar equations, we have

$$\left[\frac{k_x}{k_\perp} f_{0h}^+ + \frac{\left(-\frac{\partial g}{\partial y} k_\perp^2 + k_\perp k_{0z} \right)}{k_\perp k_0} f_{0v}^+ \right] e^{ik_{0z} g(\bar{r}_\perp)}$$

$$+\left[\frac{k_x}{k_\perp}e_0^h\delta\left(\bar{k}_\perp-\bar{k}_\perp^i\right)+\frac{\left(-\frac{\partial g}{\partial y}k_\perp^2-k_yk_{0z}\right)}{k_\perp k_0}e_0^v\delta\left(\bar{k}_\perp-\bar{k}_\perp^i\right)\right]e^{-ik_{0z}g(\bar{r}_\perp)}$$

$$=\left[\frac{k_x}{k_\perp}f_{1h}^-\mathbf{R}_1^he^{2ik_{1z}d_1}+\frac{\left(-\frac{\partial g}{\partial y}k_\perp^2+k_yk_{1z}\right)}{k_\perp k_1}f_{1v}^-\mathbf{R}_1^ve^{2ik_{1z}d_1}\right]e^{ik_{1z}g(\bar{r}_\perp)}$$

$$+\left[\frac{k_x}{k_\perp}f_{1h}^-+\frac{\left(-\frac{\partial g}{\partial y}k_\perp^2-k_yk_{1z}\right)}{k_\perp k_1}f_{1v}^-\right]e^{-ik_{1z}g(\bar{r}_\perp)} \tag{B1}$$

$$\left[\frac{k_y}{k_\perp}f_{0h}^++\frac{\left(\frac{\partial g}{\partial x}k_\perp^2-k_xk_{0z}\right)}{k_\perp k_0}f_{0v}^+\right]e^{ik_{0z}g(\bar{r}_\perp)}$$

$$+\left[\frac{k_y}{k_\perp}e_0^h\delta\left(\bar{k}_\perp-\bar{k}_\perp^i\right)+\frac{\left(\frac{\partial g}{\partial x}k_\perp^2+k_xk_{0z}\right)}{k_\perp k_0}e_0^v\delta\left(\bar{k}_\perp-\bar{k}_\perp^i\right)\right]e^{-ik_{0z}g(\bar{r}_\perp)}$$

$$=\left[\frac{k_y}{k_\perp}f_{1h}^-\mathbf{R}_1^he^{2ik_{1z}d_1}+\frac{\left(\frac{\partial g}{\partial x}k_\perp^2-k_xk_{1z}\right)}{k_\perp k_1}f_{1v}^-\mathbf{R}_1^ve^{2ik_{1z}d_1}\right]e^{ik_{1z}g(\bar{r}_\perp)}$$

$$+\left[\frac{k_y}{k_\perp}f_{1h}^-+\frac{\left(\frac{\partial g}{\partial x}k_\perp^2+k_xk_{1z}\right)}{k_\perp k_1}f_{1v}^-\right]e^{-ik_{1z}g(\bar{r}_\perp)} \tag{B2}$$

$$\frac{1}{\eta_0}\left\{\left[-\frac{\left(-\frac{\partial g}{\partial y}k_\perp^2+k_yk_{0z}\right)}{k_\perp k_0}f_{0h}^++\frac{k_x}{k_\perp}f_{0v}^+\right]e^{ik_{0z}g(\bar{r}_\perp)}\right.$$

$$\left.+\left[\frac{\left(\frac{\partial g}{\partial y}k_\perp^2+k_yk_{0z}\right)}{k_\perp k_0}e_0^h\delta\left(\bar{k}_\perp-\bar{k}_\perp^i\right)+\frac{k_x}{k_\perp}e_0^v\delta\left(\bar{k}_\perp-\bar{k}_\perp^i\right)\right]e^{-ik_{0z}g(\bar{r}_\perp)}\right\}$$

$$=\frac{1}{\eta_1}\left\{\left[-\frac{\left(-\frac{\partial g}{\partial y}k_\perp^2+k_yk_{1z}\right)}{k_\perp k_1}f_{1h}^-\mathbf{R}_1^he^{2ik_{1z}d_1}\right.\right.$$

$$\left.+\frac{k_x}{k_\perp}f_{1v}^-\mathbf{R}_1^ve^{2ik_{1z}d_1}\right]e^{ik_{1z}g(\bar{r}_\perp)}$$

$$\left.+\left[\frac{\left(\frac{\partial g}{\partial y}k_\perp^2+k_yk_{1z}\right)}{k_\perp k_1}f_{1h}^-+\frac{k_x}{k_\perp}f_{1v}^-\right]e^{-ik_{1z}g(\bar{r}_\perp)}\right\} \tag{B3}$$

$$\frac{1}{\eta_0}\left\{\left[-\frac{\left(\frac{\partial g}{\partial x}k_\perp^2-k_xk_{0z}\right)}{k_\perp k_0}f_{0h}^{+}+\frac{k_y}{k_\perp}f_{0v}^{+}\right]e^{ik_{0z}g(\bar{r}_\perp)}\right.$$
$$\left.+\left[-\frac{\left(\frac{\partial g}{\partial x}k_\perp^2+k_xk_{0z}\right)}{k_\perp k_0}e_0^h\delta\left(\bar{k}_\perp-\bar{k}_\perp^i\right)+\frac{k_y}{k_\perp}e_0^v\delta\left(\bar{k}_\perp-\bar{k}_\perp^i\right)\right]e^{-ik_{0z}g(\bar{r}_\perp)}\right\}$$

$$=\frac{1}{\eta_1}\left\{\left[-\frac{\left(\frac{\partial g}{\partial x}k_\perp^2-k_xk_{1z}\right)}{k_\perp k_1}f_{1h}^{-}\mathbf{R}_1^h e^{2ik_{1z}d_1}+\frac{k_y}{k_\perp}f_{1v}^{-}\mathbf{R}_1^v e^{2ik_{1z}d_1}\right]e^{ik_{1z}g(\bar{r}_\perp)}\right.$$
$$\left.+\left[-\frac{\left(\frac{\partial g}{\partial x}k_\perp^2+k_xk_{1z}\right)}{k_\perp k_1}f_{1h}^{-}+\frac{k_y}{k_\perp}f_{1v}^{-}\right]e^{-ik_{1z}g(\bar{r}_\perp)}\right\} \tag{B4}$$

The linear equation set has four independent equations and four unknown variables, thus the equation set has a unique solution.

APPENDIX C. THE EXPRESSIONS OF THE VECTORS $\mathbf{b}_1$ AND $\mathbf{b}_2$

The complete expression of $\mathbf{b}_1$ is

$$b_{11}=\left[iG\left(\bar{k}_\perp-\bar{k}_\perp^i\right)\right]\left[\frac{k_\perp^i}{k_0}\left(1-\frac{\varepsilon_0}{\varepsilon_1}\right)\frac{T_0^{vi}\left(1+\mathbf{R}_1^{vi}e^{2ik_{1z}^id_1}\right)}{1+R_0^{vi}\mathbf{R}_1^{vi}e^{2ik_{1z}^id_1}}k_ye_0^v\right] \tag{C1}$$

$$b_{12}=\left[iG\left(\bar{k}_\perp-\bar{k}_\perp^i\right)\right]\left[\frac{k_\perp^i}{k_0}\left(1-\frac{\varepsilon_0}{\varepsilon_1}\right)\frac{T_0^{vi}\left(1+\mathbf{R}_1^{vi}e^{2ik_{1z}^id_1}\right)}{1+R_0^{vi}\mathbf{R}_1^{vi}e^{2ik_{1z}^id_1}}\left(-k_x\right)e_0^v\right] \tag{C2}$$

$$b_{13}=\left[iG\left(\bar{k}_\perp-\bar{k}_\perp^i\right)\right]\left[\frac{k_y^i}{k_\perp^i}\left(\frac{k_0}{\eta_0}-\frac{k_1}{\eta_1}\right)\frac{T_0^{hi}\left(1+\mathbf{R}_1^{hi}e^{2ik_{1z}^id_1}\right)}{1+\mathbf{R}_0^{hi}\mathbf{R}_1^{hi}e^{2ik_{1z}^id_1}}e_0^h\right.$$
$$\left.+\frac{k_x^ik_{0z}^i}{k_\perp^i}\frac{1}{\eta_0}\frac{(\varepsilon_0-\varepsilon_1)}{\varepsilon_0}\left(1-\mathbf{R}_0^{vi}\right)\frac{\left(1-\mathbf{R}_1^{vi}e^{2ik_{1zi}d_1}\right)}{1+\mathbf{R}_0^{vi}\mathbf{R}_1^{vi}e^{2ik_{1zi}d_1}}e_0^v\right] \tag{C3}$$

$$b_{14}=\left[iG\left(\bar{k}_\perp-\bar{k}_\perp^i\right)\right]\left[-\frac{k_x^i}{k_\perp^i}\left(\frac{k_0}{\eta_0}-\frac{k_1}{\eta_1}\right)\frac{T_0^{hi}\left(1+\mathbf{R}_1^{hi}e^{2ik_{1z}^id_1}\right)}{1+\mathbf{R}_0^{hi}\mathbf{R}_1^{hi}e^{2ik_{1z}^id_1}}e_0^h\right.$$

$$+\frac{k_y^i k_{0z}^i}{k_\perp^i}\frac{1}{\eta_0}\frac{(\varepsilon_0-\varepsilon_1)}{\varepsilon_0}\left(1-\mathbf{R}_0^{vi}\right)\frac{\left(1-\mathbf{R}_1^{vi}e^{2ik_{1z}^i d_1}\right)}{1+\mathbf{R}_0^{vi}\mathbf{R}_1^{vi}e^{2ik_{1z}^i d_1}}e_0^v\Bigg] \tag{C4}$$

The complete expression of $\mathbf{b}_2$ is

$$\begin{aligned}
b_{21}=&\int d\bar{\kappa}_\perp F\left(\bar{k}_\perp-\bar{\kappa}_\perp\right)F\left(\bar{\kappa}_\perp-\bar{k}_\perp^i\right)\times\Bigg\{\Bigg[\frac{\kappa_x\kappa_{0z}}{\kappa_\perp}\tilde{f}_{0h}^{+(1)}\left(\bar{\kappa}_\perp\right)\\
&+\frac{\kappa_y\kappa_{0z}^2}{\kappa_\perp k_0}\tilde{f}_{0v}^{+(1)}\left(\bar{\kappa}_\perp\right)+\frac{\kappa_x\kappa_{1z}}{\kappa_\perp}\left(1-\mathbf{R}_1^{h\kappa}e^{2i\kappa_{1z}d_1}\right)\tilde{f}_{1h}^{-(1)}\left(\bar{\kappa}_\perp\right)\\
&-\frac{\kappa_y\kappa_{1z}^2}{\kappa_\perp k_1}\left(1+\mathbf{R}_1^{v\kappa}e^{2i\kappa_{1z}d_1}\right)\tilde{f}_{1v}^{-(1)}\left(\bar{\kappa}_\perp\right)\Bigg]+\left(k_y-\kappa_y\right)\Bigg[-\frac{\kappa_\perp}{k_0}\tilde{f}_{0v}^{+(1)}\left(\bar{\kappa}_\perp\right)\\
&+\frac{\kappa_\perp}{k_1}\left(1+\mathbf{R}_1^{v\kappa}e^{2i\kappa_{1z}d_1}\right)\tilde{f}_{1v}^{-(1)}\left(\bar{\kappa}_\perp\right)\Bigg]+\frac{1}{2}\Bigg[\frac{k_x^i {k_{0z}^i}^2}{k_\perp^i}\mathbf{R}_0^{hi}e_0^h+\frac{k_y^i {k_{0z}^i}^3}{k_\perp^i k_0}\mathbf{R}_0^{vi}e_0^v\\
&-\frac{k_x^i {k_{1z}^i}^2}{k_\perp^i}\left(1+\mathbf{R}_1^{hi}e^{2ik_{1zi}d}\right)T_0^{hi}e_0^h+\frac{k_y^i {k_{1z}^i}^3}{k_\perp^i k_1}\left(1-\mathbf{R}_1^{vi}e^{2ik_{1zi}d_1}\right)T_0^{hi}e_0^v\\
&+\frac{k_x^i {k_{0z}^i}^2}{k_\perp^i}e_0^h-\frac{k_y^i {k_{0z}^i}^3}{k_\perp^i k_0}e_0^v\Bigg]+\left(k_y-\kappa_y\right)\Bigg[-\frac{k_\perp^i k_{0z}^i}{k_0}\mathbf{R}_0^{vi}e_0^v\\
&-\frac{k_\perp^i k_{1z}^i}{k_1}\left(1-\mathbf{R}_1^{vi}e^{2ik_{1zi}d_1}\right)T_0^{hi}e_0^v+\frac{k_\perp^i k_{0z}^i}{k_0}e_0^v\Bigg]\Bigg\}
\end{aligned} \tag{C5}$$

$$\begin{aligned}
b_{22}=&\int d\bar{\kappa}_\perp F\left(\bar{k}_\perp-\bar{\kappa}_\perp\right)F\left(\bar{\kappa}_\perp-\bar{k}_\perp^i\right)\times\Bigg\{\Bigg[\frac{\kappa_y\kappa_{0z}}{\kappa_\perp}\tilde{f}_{0h}^{+(1)}\left(\bar{\kappa}_\perp\right)\\
&-\frac{\kappa_x\kappa_{0z}^2}{\kappa_\perp k_0}\tilde{f}_{0v}^{+(1)}\left(\bar{\kappa}_\perp\right.+\frac{\kappa_y\kappa_{1z}}{\kappa_\perp}\left(1-\mathbf{R}_1^{h\kappa}e^{2i\kappa_{1z}d_1}\right)\tilde{f}_{1h}^{-(1)}\left(\bar{\kappa}_\perp\right)\\
&+\frac{\kappa_x\kappa_{1z}^2}{\kappa_\perp k_1}\left(1+\mathbf{R}_1^{v\kappa}e^{2i\kappa_{1z}d_1}\right)\tilde{f}_{1v}^{-(1)}\left(\bar{\kappa}_\perp\right)\Bigg]+\left(k_x-\kappa_x\right)\Bigg[\frac{\kappa_\perp}{k_0}\tilde{f}_{0v}^{+(1)}\left(\bar{\kappa}_\perp\right)\\
&-\frac{\kappa_\perp}{k_1}\left(1+\mathbf{R}_1^{v\kappa}e^{2i\kappa_{1z}d_1}\right)\tilde{f}_{1v}^{-(1)}\left(\bar{\kappa}_\perp\right)\Bigg]+\frac{1}{2}\Bigg[\frac{k_y^i {k_{0z}^i}^2}{k_\perp^i}\mathbf{R}_0^{hi}e_0^h\\
&-\frac{k_x^i {k_{0z}^i}^3}{k_\perp^i k_0}\mathbf{R}_0^{vi}e_0^v-\frac{k_y^i {k_{1z}^i}^2}{k_{\rho i}}\left(1+\mathbf{R}_1^{hi}e^{2ik_{1zi}d_1}\right)T_0^{hi}e_0^h\\
&-\frac{k_x^i {k_{1z}^i}^3}{k_\perp^i k_1}\left(1-\mathbf{R}_1^{vi}e^{2ik_{1zi}d_1}\right)T_0^{hi}e_0^v+\frac{k_y^i {k_{0z}^i}^2}{k_\perp^i}e_0^h+\frac{k_x^i {k_{0z}^i}^3}{k_\perp^i k_0}e_0^v\Bigg]+\left(k_x-\kappa_x\right)\\
&\Bigg[\frac{k_\perp^i k_{0z}^i}{k_0}\mathbf{R}_0^{vi}e_0^v+\frac{k_\perp^i k_{1z}^i}{k_1}\left(1-\mathbf{R}_1^{vi}e^{2ik_{1zi}d_1}\right)T_0^{hi}e_0^v-\frac{k_\perp^i k_{0z}^i}{k_0}e_0^v\Bigg]\Bigg\}
\end{aligned} \tag{C6}$$

$$
\begin{aligned}
b_{23} = &\int d\bar{\kappa}_\perp F\left(\bar{k}_\perp - \bar{\kappa}_\perp\right) F\left(\bar{\kappa}_\perp - \bar{k}^i_\perp\right) \times \Bigg\{ \Bigg[-\frac{\kappa_y \kappa_{0z}^2}{\eta_0 \kappa_\perp k_0} \tilde{f}_{0h}^{+(1)}\left(\bar{\kappa}_\perp\right) \\
&+ \frac{\kappa_x \kappa_{0z}}{\eta_0 \kappa_\perp} \tilde{f}_{0v}^{+(1)}\left(\bar{\kappa}_\perp\right) + \frac{\kappa_y \kappa_{1z}^2}{\eta_1 \kappa_\perp k_1}\left(1 + \mathbf{R}_1^{h\kappa} e^{2i\kappa_{1z} d_1}\right) \tilde{f}_{1h}^{-(1)}\left(\bar{\kappa}_\perp\right) \\
&+ \frac{\kappa_x \kappa_{1z}}{\eta_1 \kappa_\perp}\left(1 - \mathbf{R}_1^{v\kappa} e^{2i\kappa_{1z} d_1}\right) \tilde{f}_{1v}^{-(1)}\left(\bar{\kappa}_\perp\right)\Bigg] + \left(k_y - \kappa_y\right)\Bigg[\frac{\kappa_\perp}{\eta_0 k_0} \tilde{f}_{0h}^{+(1)}\left(\bar{\kappa}_\perp\right) \\
&- \frac{\kappa_\perp}{\eta_1 k_1}\left(1 + \mathbf{R}_1^{h\kappa} e^{2i\kappa_{1z} d_1}\right) \tilde{f}_{1h}^{-(1)}\left(\bar{\kappa}_\perp\right)\Bigg] + \frac{1}{2}\Bigg[-\frac{k_y^i {k_{0z}^i}^3}{\eta_0 k_\perp^i k_0} \mathbf{R}_0^{hi} e_0^h \\
&+ \frac{k_x^i {k_{0z}^i}^2}{\eta_0 k_\perp^i} \mathbf{R}_0^{vi} e_0^v - \frac{k_y^i {k_{1z}^i}^3}{\eta_1 k_\perp^i k_1}\left(1 - \mathbf{R}_1^{hi} e^{2ik_{1zi} d_1}\right) T_0^{hi} e_0^h \\
&- \frac{k_x^i {k_{1z}^i}^2}{\eta_1 k_\perp^i}\left(1 + \mathbf{R}_1^{vi} e^{2ik_{1zi} d_1}\right) T_0^{hi} e_0^v + \frac{k_y^i {k_{0z}^i}^3}{\eta_0 k_\perp^i k_0} e_0^h + \frac{k_x^i {k_{0z}^i}^2}{\eta_0 k_\perp^i} e_0^v\Bigg] + \left(k_y - \kappa_y\right) \\
&\Bigg[\frac{k_\perp^i k_{0z}^i}{\eta_0 k_0} \mathbf{R}_0^{hi} e_0^h + \frac{k_\perp^i k_{1z}^i}{\eta_1 k_1}\left(1 - \mathbf{R}_1^{hi} e^{2ik_{1zi} d_1}\right) T_0^{hi} e_0^h - \frac{k_\perp^i k_{0z}^i}{\eta_0 k_0} e_0^h\Bigg]\Bigg\} \qquad \text{(C7)}
\end{aligned}
$$

$$
\begin{aligned}
b_{24} = &\int d\bar{\kappa}_\perp F\left(\bar{k}_\perp - \bar{\kappa}_\perp\right) F\left(\bar{\kappa}_\perp - \bar{k}^i_\perp\right) \times \Bigg\{ \Bigg[\frac{\kappa_x \kappa_{0z}^2}{\eta_0 \kappa_\perp k_0} \tilde{f}_{0h}^{+(1)}\left(\bar{\kappa}_\perp\right) \\
&+ \frac{\kappa_y \kappa_{0z}}{\eta_0 \kappa_\perp} \tilde{f}_{0v}^{+(1)}\left(\bar{\kappa}_\perp\right) - \frac{\kappa_x \kappa_{1z}^2}{\eta_1 \kappa_\perp k_1}\left(1 + \mathbf{R}_1^{h\kappa} e^{2i\kappa_{1z} d_1}\right) \tilde{f}_{1h}^{-(1)}\left(\bar{\kappa}_\perp\right) \\
&+ \frac{\kappa_y \kappa_{1z}}{\eta_1 \kappa_\perp}\left(1 - \mathbf{R}_1^{v\kappa} e^{2i\kappa_{1z} d_1}\right) \tilde{f}_{1v}^{-(1)}\left(\bar{\kappa}_\perp\right)\Bigg] + \left(k_x - \kappa_x\right)\Bigg[-\frac{\kappa_\perp}{\eta_0 k_0} \tilde{f}_{0h}^{+(1)}\left(\bar{\kappa}_\perp\right) \\
&+ \frac{\kappa_\perp}{\eta_1 k_1}\left(1 + \mathbf{R}_1^{h\kappa} e^{2i\kappa_{1z} d_1}\right) \tilde{f}_{1h}^{-(1)}\left(\bar{\kappa}_\perp\right)\Bigg] + \frac{1}{2}\Bigg[\frac{k_x^i {k_{0z}^i}^3}{\eta_0 k_\perp^i k_0} \mathbf{R}_0^{hi} e_0^h + \\
&\frac{k_y^i {k_{0z}^i}^2}{\eta_0 k_\perp^i} \mathbf{R}_0^{vi} e_0^v + \frac{k_x^i {k_{1z}^i}^3}{\eta_1 k_\perp^i k_1}\left(1 - \mathbf{R}_1^{hi} e^{2ik_{1zi} d_1}\right) T_0^{hi} e_0^h \\
&- \frac{k_y^i {k_{1z}^i}^2}{\eta_1 k_\perp^i}\left(1 + \mathbf{R}_1^{vi} e^{2ik_{1zi} d_1}\right) T_0^{hi} e_0^v \\
&- \frac{k_x^i {k_{0z}^i}^3}{\eta_0 k_\perp^i k_0} e_0^h + \frac{k_y^i {k_{0z}^i}^2}{\eta_0 k_\perp^i} e_0^v\Bigg] + \left(k_x - \kappa_x\right) \\
&\Bigg[-\frac{k_\perp^i k_{0z}^i}{\eta_0 k_0} \mathbf{R}_0^{hi} e_0^h - \frac{k_\perp^i k_{1z}^i}{\eta_1 k_1}\left(1 - \mathbf{R}_1^{hi} e^{2ik_{1zi} d_1}\right) T_0^{hi} e_0^h + \frac{k_\perp^i k_{0z}^i}{\eta_0 k_0} e_0^h\Bigg]\Bigg\} \qquad \text{(C8)}
\end{aligned}
$$

where the parameters with superscript κ are functions of the dummy variable $\bar{\kappa}_\perp$.

APPENDIX D. THE DETAIL EXPRESSIONS OF THE FIRST- AND SECOND-ORDER SPM SOLUTIONS

The detail expressions of $\tilde{f}_{0pp}^{+(1)}$, $\tilde{f}_{0pq}^{+(1)}$, $\tilde{f}_{1pp}^{-(1)}$ and $\tilde{f}_{1pq}^{-(1)}$ are

$$\tilde{f}_{0hh}^{+(1)} = \frac{k_0(\varepsilon_1-\varepsilon_0)}{2\varepsilon_0}\frac{\cos\left(\phi-\phi^i\right)}{\cos\theta}\left(1+\mathbf{R}_0^h\right)\left(1+\mathbf{R}_0^{hi}\right)e_0^h \tag{D1}$$

$$\tilde{f}_{0hv}^{+(1)} = \frac{k_0(\varepsilon_1-\varepsilon_0)}{2\varepsilon_0}\frac{\sin\left(\phi-\phi^i\right)\cos\theta^i}{\cos\theta}\left(1+\mathbf{R}_0^h\right)\left(1-\mathbf{R}_0^{vi}\right)e_0^v \tag{D2}$$

$$\tilde{f}_{0vh}^{+(1)} = \frac{k_0(\varepsilon_1-\varepsilon_0)}{2\varepsilon_0}\sin\left(\phi-\phi^i\right)\left(1+\mathbf{R}_0^{hi}\right)\left(1-\mathbf{R}_0^v\right)e_0^h \tag{D3}$$

$$\begin{aligned}\tilde{f}_{0vv}^{+(1)} =& \frac{k_0(\varepsilon_1-\varepsilon_0)}{2\varepsilon_1}\frac{\sin\theta\sin\theta^i}{\cos\theta}\left(1+\mathbf{R}_0^{vi}\right)\left(1+\mathbf{R}_0^v\right)e_0^v \\ &-\frac{k_0(\varepsilon_1-\varepsilon_0)}{2\varepsilon_0}\cos\left(\phi-\phi^i\right)\cos\theta^i\left(1-\mathbf{R}_0^{vi}\right)\left(1-\mathbf{R}_0^v\right)e_0^v\end{aligned} \tag{D4}$$

$$\tilde{f}_{1hh}^{+(1)} = \frac{k_0(\varepsilon_1-\varepsilon_0)}{2\varepsilon_0}\frac{\cos\left(\phi-\phi^i\right)}{\cos\theta}\left(1+\mathbf{R}_0^{hi}\right)T_0^h e_0^h \tag{D5}$$

$$\tilde{f}_{1hv}^{+(1)} = \frac{k_0(\varepsilon_1-\varepsilon_0)}{2\varepsilon_0}\frac{\sin\left(\phi-\phi^i\right)\cos\theta^i}{\cos\theta}\left(1-\mathbf{R}_0^{vi}\right)T_0^h e_0^v \tag{D6}$$

$$\tilde{f}_{1vh}^{+(1)} = -\frac{k_1(\varepsilon_1-\varepsilon_0)}{2\varepsilon_1}\sin\left(\phi-\phi^i\right)\left(1+\mathbf{R}_0^{hi}\right)T_0^v e_0^h \tag{D7}$$

$$\begin{aligned}\tilde{f}_{1vv}^{+(1)} =& \frac{k_1(\varepsilon_1-\varepsilon_0)}{2\varepsilon_1}\cos\left(\phi-\phi^i\right)\cos\theta^i\left(1-\mathbf{R}_0^{vi}\right)T_0^v e_0^v \\ &+\frac{k_1(\varepsilon_1-\varepsilon_0)}{2\varepsilon_1}\frac{\varepsilon_0}{\varepsilon_1}\tan\theta\sin\theta^i\left(1+\mathbf{R}_0^{vi}\right)T_0^v e_0^v\end{aligned} \tag{D8}$$

where $\left(\theta^i,\phi^i\right)$ and (θ,ϕ) are the incident and scattering azimuth angles respectively.

The detailed expressions of $f_{0pq}^{+(2)}$, $p,q=H,V$ are

$$f_{0pq}^{+(2)} = \int_{-\infty}^{+\infty} d\bar{\kappa}_\perp G\left(\bar{k}_\perp-\bar{\kappa}_\perp\right)G\left(\bar{\kappa}_\perp-\bar{k}_\perp^i\right)\tilde{f}_{0pq}^{+(2)}\left(\bar{\kappa}_\perp\right) \tag{D9}$$

$$\tilde{f}_{0pq}^{+(2)}\left(\bar{\kappa}_\perp\right) = \tilde{c}_{pq}+\tilde{d}_{pq}\left(\bar{\kappa}_\perp\right) \tag{D10}$$

where

$$\tilde{c}_{hh} = \frac{1}{4}\left(k_1^2-k_0^2\right)\cos\left(\phi-\phi^i\right)\left[\left(1+\mathbf{R}_0^{hi}\right)\left(1-\mathbf{R}_0^h\right)\right.$$

$$+\frac{\cos\theta^i}{\cos\theta}\left(1-\mathbf{R}_0^{hi}\right)\left(1+\mathbf{R}_0^{h}\right)\Big] \tag{D11}$$

$$\begin{aligned}
\tilde{d}_{hh}\left(\bar{\kappa}_\perp\right) &= -\frac{1}{4}\left(1+\mathbf{R}_0^{h}\right)\left(1+\mathbf{R}_0^{hi}\right)\frac{\left(k_1^2-k_0^2\right)^2}{k_0^2}\frac{1}{\cos\theta}\\
&\quad\left[\frac{\cos\left(\phi-\phi^\kappa\right)\cos\left(\phi^\kappa-\phi^i\right)}{\cos\theta^\kappa}\left(1+\mathbf{R}_0^{h\kappa}\right)\right.\\
&\quad\left.-\sin\left(\phi^\kappa-\phi^i\right)\sin\left(\phi-\phi^\kappa\right)\cos\theta^\kappa\left(1-\mathbf{R}_0^{v\kappa}\right)\right]
\end{aligned}\tag{D12}$$

$$\begin{aligned}
\tilde{c}_{hv} &= \frac{1}{4}\left(k_1^2-k_0^2\right)\sin\left(\phi-\phi^i\right)\left[\cos\theta^i\left(1-\mathbf{R}_0^{vi}\right)\left(1-\mathbf{R}_0^{h}\right)\right.\\
&\quad\left.+\frac{1}{\cos\theta}\left(1+\mathbf{R}_0^{vi}\right)\left(1+\mathbf{R}_0^{h}\right)\right]
\end{aligned}\tag{D13}$$

$$\begin{aligned}
\tilde{d}_{hv}\left(\bar{\kappa}_\perp\right) &= -\frac{1}{4\cos\theta}\left(k_1^2-k_0^2\right)\times\left\{\sin\left(\phi-\phi^\kappa\right)\right.\\
&\quad\sin\theta^\kappa\sin\theta^i\left(1+\mathbf{R}_0^{vi}\right)\left(1+\mathbf{R}_0^{h}\right)\frac{1}{k_1^2}\left[k_0^2\left(1+\mathbf{R}_0^{v\kappa}\right)\right.\\
&\quad\left.+k_1^2\left(1-\mathbf{R}_0^{v\kappa}\right)\right]+\cos\left(\phi-\phi^\kappa\right)\sin\left(\phi^\kappa-\phi^i\right)\frac{1}{\cos\theta^\kappa}\\
&\quad\cos\theta^i\frac{\left(k_1^2-k_0^2\right)}{k_0^2}\left(1-\mathbf{R}_0^{vi}\right)\left(1+\mathbf{R}_0^{h}\right)\left(1+\mathbf{R}_0^{h\kappa}\right)\\
&\quad+\sin\left(\phi-\phi^\kappa\right)\cos\left(\phi^\kappa-\phi^i\right)\cos\theta^\kappa\cos\theta^i\frac{\left(k_1^2-k_0^2\right)}{k_0^2}\\
&\quad\left.\left(1-\mathbf{R}_0^{vi}\right)\left(1-\mathbf{R}_0^{h}\right)\left(1-\mathbf{R}_0^{v\kappa}\right)\right\}
\end{aligned}\tag{D14}$$

$$\begin{aligned}
\tilde{c}_{vh} &= \frac{1}{4}\left(k_1^2-k_0^2\right)\sin\left(\phi-\phi^i\right)\left[\frac{1}{\cos\theta}\left(1+\mathbf{R}_0^{hi}\right)\left(1+\mathbf{R}_0^{v}\right)\right.\\
&\quad\left.+\cos\theta^i\left(1-\mathbf{R}_0^{hi}\right)\left(1-\mathbf{R}_0^{v}\right)\right]
\end{aligned}\tag{D15}$$

$$\begin{aligned}
\tilde{d}_{vh}\left(\bar{\kappa}_\perp\right) &= -\frac{1}{4\cos\theta}\left(k_1^2-k_0^2\right)\times\left\{\sin\left(\phi^\kappa-\phi^i\right)\right.\\
&\quad\sin\theta\sin\theta^\kappa\left(1+\mathbf{R}_0^{hi}\right)\left[1+\mathbf{R}_0^{v}\right]\frac{1}{k_1^2}\left[k_0^2\left(1+\mathbf{R}_0^{v\kappa}\right)\right.\\
&\quad\left.+k_1^2\left(1-\mathbf{R}_0^{v\kappa}\right)\right]+\sin\left(\phi-\phi^\kappa\right)\cos\left(\phi^\kappa-\phi^i\right)\\
&\quad\frac{\cos}{\theta}\frac{1}{\cos\theta^\kappa}k_1^2-k_0^2k_0^2\left(1+\mathbf{R}_0^{hi}\right)\left(1-\mathbf{R}_0^{v}\right)\left(1+\mathbf{R}_0^{h\kappa}\right)\\
&\quad+\cos\left(\phi-\phi^\kappa\right)\sin\left(\phi^\kappa-\phi^i\right)\cos\theta\cos\theta^\kappa\frac{k_1^2-k_0^2}{k_0^2}
\end{aligned}$$

$$\left(1+\mathbf{R}_0^{hi}\right)\left(1-\mathbf{R}_0^{v}\right)\left(1-\mathbf{R}_0^{v\kappa}\right)\Big\} \tag{D16}$$

$$\begin{aligned}\tilde{c}_{vv} &= -\frac{1}{4}\left(k_1^2-k_0^2\right)\cos\left(\phi-\phi^i\right)\left[\frac{k_{0zi}}{k_{0z}}\left(1-\mathbf{R}_0^{vi}\right)\left(1+\mathbf{R}_0^{v}\right)\right.\\ &\quad \left.+\left(1+\mathbf{R}_0^{vi}\right)\left(1-\mathbf{R}_0^{v}\right)\right]\end{aligned} \tag{D17}$$

$$\begin{aligned}\tilde{d}_{vv}\left(\bar{\kappa}_\perp\right) &= \frac{1}{4}\left(1-\mathbf{R}_0^{v}\right)\times\left[-\sin\left(\phi-\phi^\kappa\right)\right.\\ &\quad \sin\left(\phi^\kappa-\phi^i\right)\cos\theta^i\frac{1}{\cos\theta^\kappa}\left(k_1^2-k_0^2\right)^2\frac{1}{k_0^2}\left(1-\mathbf{R}_0^{vi}\right)\\ &\quad \left(1+\mathbf{R}_0^{h\kappa}\right)+\cos\left(\phi-\phi^\kappa\right)\sin\theta^\kappa\sin\theta^i\left(k_1^2-k_0^2\right)\\ &\quad \left(1+\mathbf{R}_0^{vi}\right)k_0^2\left(\frac{1+\mathbf{R}_0^{v\kappa}}{k_1^2}+\frac{1-\mathbf{R}_0^{v\kappa}}{k_0^2}\right)\\ &\quad +\cos\left(\phi-\phi^\kappa\right)\cos\left(\phi^\kappa-\phi^i\right)\cos\theta^\kappa\cos\theta^i\left(k_1^2-k_0^2\right)^2\\ &\quad \left.\frac{1}{k_0^2}\left(1-\mathbf{R}_0^{vi}\right)\left(1-\mathbf{R}_0^{v\kappa}\right)\right]+\frac{1}{4}\tan\theta\sin\theta^\kappa k_0^2\left(1+\mathbf{R}_0^{v}\right)\\ &\quad \times\left[-\tan\theta^\kappa\sin\theta^i\left(\frac{k_1^2-k_0^2}{k_1^2}\right)^2\left(1+\mathbf{R}_0^{vi}\right)\left(1+\mathbf{R}_0^{v\kappa}\right)\right.\\ &\quad +\cos\left(\phi^\kappa-\phi^i\right)\cos\theta^i\left(k_1^2-k_0^2\right)\left(1-\mathbf{R}_0^{vi}\right)\\ &\quad \left.\left(\frac{1+\mathbf{R}_0^{v\kappa}}{k_1^2}+\frac{1-\mathbf{R}_0^{v\kappa}}{k_0^2}\right)\right]\end{aligned} \tag{D18}$$

The parameters with superscript κ in the above expressions refer to the dummy variable $\bar{\kappa}_\perp$. We see the expressions of $\tilde{f}_{0pq}^{+(2)}\left(\bar{\kappa}_\perp\right)$, $\tilde{f}_{0pq}^{+(2)}\left(\bar{\kappa}_\perp\right)$, $\tilde{f}_{0pq}^{+(2)}\left(\bar{\kappa}_\perp\right)$ and $\tilde{f}_{0pq}^{+(2)}\left(\bar{\kappa}_\perp\right)$ exhibit symmetry of reciprocity.

REFERENCES

1. Franceschini, G., A. Abubakar, T. M. Habashy, et al., "A comparative assessment among iterative linear solvers dealing with electromagnetic integral equations in 3D inhomogeneous anisotropic media," *Journal of Electromagnetic Waves and Applications*, Vol. 21, No. 7, 899–914, 2007.
2. Zhang, H., S. Y. Tan, and H. S. Tan, "An improved method for microwave nondestructive dielectric measurement of layered media," *Progress In Electromagnetics Research B*, Vol. 10, 145–161, 2008.

3. Popov, A. V. and V. V. Kopeikin, "Electromagnetic pulse propagation over nonuniform earth surface: Numerical simulation," *Progress In Electromagnetics Research B*, Vol. 6, 37–64, 2008.
4. Hichem, N. and T. Aguili, "Scattering by multilayered structures using the extended method of auxiliary sources EMAS," *Progress In Electromagnetics Research B*, Vol. 15, 133–150, 2009.
5. Wang, R. and L.-X. Guo, "Numerical simulations of wave scattering from two-layered rough interface," *Progress In Electromagnetics Research B*, Vol. 10, 163–175, 2008.
6. Fuks, I. M., "Wave diffraction by a rough boundary of an arbitrary plane-layered medium," *IEEE Transactions on Antenna and Propagation*, Vol. 49, No. 4, 630–639, 2001.
7. Azadegan, R. and K. Sarabandi, "Analytical formulation of the scattering by a slightly rough dielectric boundary covered with a homogenous dielectric layer," *IEEE Antennas and Propagation Society International Symposium*, Vol. 3, 420–423, 2003.
8. Franceschetti, G., P. Imperatore, A. Iodice, et al., "Scattering from layered structures with one rough interface: A unified formulation of perturbative solutions," *IEEE Transaction on Geoscience and Remote Sensing*, Vol. 46, No. 6, 1634–1643, 2008.
9. Imperatore, P., A. Iodice, and D. Riccio, "Electromagnetic wave scattering from layered structures with an arbitrary number of rough interfaces," *IEEE Transaction on Geoscience and Remote Sensing*, Vol. 47, No. 4, 1056–1072, 2009.
10. Tabatabaeenejad, A. and M. Moghaddam, "Bistatic scattering from three-dimensional layered rough surfaces, interfaces," *IEEE Transaction on Geoscience and Remote Sensing*, Vol. 44, No. 8, 2102–2114, 2006.
11. Hajnsek, I., E. Pottier, and S. R. Cloude, "Inversion of surface parameters from polarimetric SAR," *IEEE Transaction on Geoscience and Remote Sensing*, Vol. 41, No. 4, 727–744, 2003.
12. Tsang, L. and J. A. Kong, *Scattering of Electromagnetic Waves Advanced Topics*, Wiley, 2001.
13. Johnson, J. T., "Third-order small-perturbation method for scattering from dielectric rough surfaces," *J. Opt. Soc. Am. A*, Vol. 16, No. 11, 2720–2736, 1999.
14. Greffet, J. J., "Theoretical model of the shift of the brewster angle on a rough surface," *Optical Letters*, Vol. 17, No. 4, 238–240, 1992.